

# A lateral optical equilibrium in waveguide-resonator optical force

Varat Intaraprasong,<sup>1</sup> and Shanhui Fan<sup>1\*</sup>

<sup>1</sup>*Ginzton Laboratory, Stanford University, Stanford, California 94305*

[\\*shanhui@stanford.edu](mailto:shanhui@stanford.edu)

**Abstract:** We consider the lateral optical force between a resonator and a waveguide, and study the possibility of an equilibrium that occurs solely from the optical force in such system. We prove analytically that a single-resonance system cannot give such an equilibrium in the resonator-waveguide force. We then show that two-resonance systems can provide such an equilibrium. We provide an intuitive way to predict the existence of an equilibrium, and give numerical examples.

© 2013 Optical Society of America

**OCIS codes:** (230.4555) Coupled resonators (350.4855); Optical tweezers or optical manipulation.

---

## References and links

1. D. Van Thourhout, and J. Roels, "Optomechanical device actuation through the optical gradient force," *Nat. Photonics* **4**, 211-217 (2010).
2. P. T. Rakich, P. Davids, and Z. Wang, "Tailoring optical forces in waveguides through radiation pressure and electrostrictive forces," *Opt. Express* **18**, 14439-14453 (2010).
3. V. Liu, M. Povinelli, and S. Fan, "Resonance-enhanced optical forces between coupled photonic crystal slabs," *Opt. Express* **17**, 21897-21909 (2009).
4. W.H.P. Pernice, M. Li, K. Y. Fong, and H. X. Tang, "Modeling of the optical force between propagating light-waves in parallel 3D waveguides," *Opt. Express* **7**, 16032-16037 (2009).
5. J. Roels, I. De Vlaminck, L. Lagae, B. Maes, D. Van Thourhout, and R. Baets, "Tunable optical forces between nanophotonic waveguides," *Nat. Nanotechnol.* **4**, 510-513 (2009).
6. W. H. P. Pernice, M. Li, D. Garcia-Sanchez, and H. X. Tang, "Analysis of short range forces in opto-mechanical devices with a nanogap," *Opt. Express* **18**, 12615-12621 (2010).
7. M. L. Povinelli, M. Loncar, M. Ibanescu, E. J. Smythe, S. G. Johnson, F. Capasso, and J. D. Joannopoulos, "Evanescent-wave bonding between optical waveguides," *Opt. Lett.* **30**, 3042-3044 (2005).
8. M. Li, W. H. P. Pernice, and H. X. Tang, "Tunable bipolar optical interactions between guided lightwaves," *Nat. Photonics* **3**, 464-468 (2009).
9. V. Intaraprasong, and S. Fan, "Nonvolatile bistable all-optical switch from mechanical buckling," *Appl. Phys. Lett.* **98**, 241104 (2011).
10. A. Einat, and U. Levy, "Analysis of the optical force in the micro ring resonator," *Opt. Express* **19**, 20405-20419 (2011).
11. V. Intaraprasong, and S. Fan, "Enhancing the waveguide-resonator optical force with an all-optical on-chip analog of electromagnetically induced transparency," *Phys. Rev. A* **86**, 063833 (2012).
12. M. Eichenfield, C. P. Michael, R. Perahia, and O. Painter, "Actuation of micro-optomechanical systems via cavity-enhanced optical dipole forces," *Nat. Photonics* **1**, 416-422 (2007).
13. M. Li, W. H. P. Pernice, and H. X. Tang, "Reactive cavity optical force on microdisk-coupled nanomechanical beam waveguides," *Phys. Rev. Lett.* **103**, 223901 (2009).
14. M. L. Povinelli, S. G. Johnson, M. Loncar, M. Ibanescu, E. J. Smythe, F. Capasso, and J. D. Joannopoulos, "High-Q enhancement of attractive and repulsive optical forces between coupled whispering-gallery-mode resonators," *Opt. Express* **13**, 8286-8295 (2005).
15. P. T. Rakich, M. A. Popovic, M. Soljagic, and E. P. Ippen, "Trapping, corralling and spectral bonding of optical resonances through optically induced potentials," *Nat. Photonics* **1**, 658-665 (2007).
16. J. Rosenberg, Q. Lin, and O. Painter, "Static and dynamic wavelength routing via the gradient optical force," *Nat. Photonics* **3**, 478-483 (2009).

17. G. S. Wiederhecker, L. Chen, A. Gondarenk, and M. Lipson, "Controlling photonic structures using optical forces," *Nature* **462**, 633-636 (2009).
  18. G. S. Wiederhecker, S. Manipatruni, S. Lee, and M. Lipson, "Broadband tuning of optomechanical cavities," *Opt. Express* **19**, 2782-2790 (2011).
  19. T. J. Kippenberg, and K. J. Vahala, "Cavity Opto-Mechanics," *Opt. Express* **15**, 17172-17205 (2007).
  20. M. Eichenfield, R. Camacho, J. Chan, K. J. Vahala, and O. Painter, "A picogram- and nanometre-scale photonic-crystal optomechanical cavity," *Nature* **459**, 550-555 (2009).
  21. H. A. Haus, *Waves and Fields in Optoelectronics* (Prentice-Hall, Englewood Cliffs, 1984).
  22. P. T. Rakich, M. A. Popovic, and Z. Wang, "General treatment of optical forces and potentials in mechanically variable photonic systems," *Opt. Express* **17**, 18116-18135 (2009).
  23. [www.comsol.com](http://www.comsol.com)
- 

## 1. Introduction

There have been significant recent interests on the optical force in photonic nano-structures [1–18], such as coupled waveguides systems [4–9], coupled resonator-waveguide systems [10–13], or coupled resonators systems [14–18]. In many cases, the optical force is strong enough to change the static mechanical configurations of photonic nanostructures [7–9, 12, 15–18]. As one set of examples we note the demonstrations of the bending of optical waveguides, either by the optical force between two parallel waveguides [7–9], or the force between a resonator and a feeding waveguide [12]. Another example is the change in the separation between two coupled resonators due to the optical force between them [15–18]. These changes in mechanical configurations can be used to optically tune the systems' frequency response [8, 12, 16–18], to corral the resonators into an optical equilibrium [15], as a basis for a non-volatile optical memory [9], or to couple light with mechanical modes [13, 19, 20].

In most of the aforementioned systems, at each operating point, the optical force is non-vanishing, i.e. it is either attractive or repulsive but never zero. The equilibrium points of structures are set by the balance between the force due to the optical fields, and the forces that are purely mechanical in origin [7–9, 12, 15–18]. One may refer to such an equilibrium between an optical and a mechanical force as an "optomechanical equilibrium." It is interesting to explore whether it is possible to achieve an equilibrium in these optical systems just by using the optical force alone. We refer to such an equilibrium that arises purely by using an optical force alone as an "optical equilibrium" for the rest of the paper. [15] has shown that it is indeed possible to achieve such a pure optical equilibrium between two optical resonators; for a given operating frequency, the optical force has an equilibrium point; the optical force is repulsive for a small separation between the two resonators, and attractive for a large separation. Unlike an optomechanical equilibrium, where the equilibrium position depends on the power of the incident light, in an optical equilibrium, the equilibrium position is independent of the power of the incident light. Therefore, achieving an optical equilibrium enables the creation of novel optical circuits that are self-tuned and self-stabilized [15].

In this paper, we consider the possibility of creating an optical equilibrium in the waveguide-resonator optical system. We analytically and numerically study the lateral force in the system of a resonator side-coupled to a feeding waveguide (example in Fig. 1(a)). The focus of our study is on the equilibrium in the lateral force ( $y$ -direction), but we will also briefly discuss the force along the  $x$ -direction, and, for an extension of three-dimensional system, the force along the  $z$ -direction. We find that a lateral optical equilibrium cannot occur if the resonator supports only a single resonance in the vicinity of the operating frequency. Instead, in order to have an equilibrium, the system has to have at least two resonances that overlap in frequency. We provide detailed discussion of the requirements of these resonances in order to create an optical equilibrium in the waveguide-resonator systems.

This paper is organized as follows. In Sec. 2, we analyze a waveguide-resonator system where the resonator supports a single resonance, and show analytically that no optical equilib-

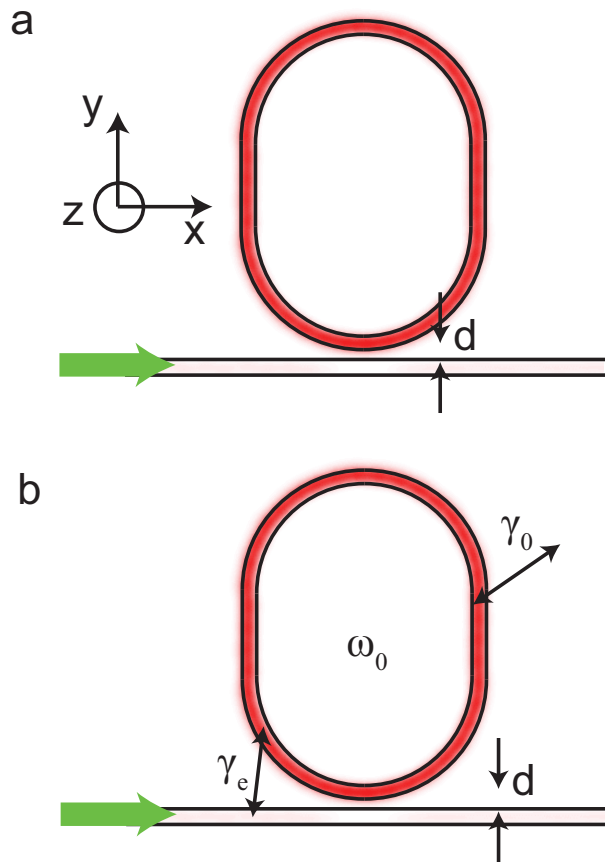


Fig. 1. (a) Schematic for a travelling-wave ring resonator. The ring and the waveguide are  $0.2\mu\text{m}$  wide. The radius of the semi-circular part of the resonator is  $1.5\mu\text{m}$  and the straight section is  $1.1\mu\text{m}$  long. The waveguide and the resonator have permittivity of 12.1 and are surrounded by air with permittivity of 1. The red color shows the local light intensity (proportional to the square of the electric field). (b) Schematic of a general resonator-waveguide system. The resonator has a single resonance at  $\omega_0$ . The incident light enters the input waveguide on the port marked with a big green arrow. The coupling rate between the resonator and the input waveguide is  $\gamma_e$ . The resonator has an intrinsic loss rate of  $\gamma_0$ .

rium can occur. We then verify this analysis with numerical simulations. In Sec. 3, we proceed to two-resonance systems and explain intuitively how to achieve an optical equilibrium in these systems. We also provide simulation results of two-resonance systems which confirm our intuitive arguments. We conclude in Sec. 4.

## 2. The lack of an optical equilibrium in single-resonance systems

### 2.1. Theory

In this section, we first review the theory of the waveguide-resonator force in a single-resonance system by deriving an analytic expression for the optical force as a function of the couplings and the resonance frequency. Then, we study the existence of the optical equilibrium by studying

how the force changes as a function of the distance between the resonator and the waveguide.

To describe the system in Fig. 1(a) we consider the model as depicted in Fig. 1(b). In this model, the resonator has a single resonance at the resonance frequency of  $\omega_0$ . The light, at a frequency  $\omega$ , enters the system through the waveguide, which couples to the resonator with a coupling constant  $\gamma_e$ . The light can exit from the resonator to the output port of the waveguide. The light can also dissipate through any loss mechanism such as material loss or radiation loss, with the loss rate  $\gamma_0$ . We will focus on the optical force between the input waveguide and the resonator. By using the coupled-mode theory for a travelling-wave resonance [21], the field enhancement factor  $\eta$  (the ratio between the resonator and input field) and the transmission coefficient  $t$  (the ratio between the output and input field) are found to be

$$\eta = e^{i\theta_1} \frac{\sqrt{2\gamma_e/t_r}}{i\Delta + \gamma_0 + \gamma_e} \quad (1)$$

$$t = e^{i\theta_2} \frac{i\Delta + \gamma_0 - \gamma_e}{i\Delta + \gamma_0 + \gamma_e} \quad (2)$$

where  $\Delta = \omega - \omega_0$ ,  $t_r$  is the round trip time in the resonator, and  $\theta_1$  and  $\theta_2$  are arbitrary phase factors depending on the positions along the waveguide where the fields are measured.

In order to find the optical force  $F$  between the input waveguide and the resonator in this system, we use the theory in [22],

$$F = -\frac{1}{\omega} \sum_i P_i \frac{\partial}{\partial d} \phi_i \quad (3)$$

where  $P_i$  is the power at each exit channel,  $\phi_i$  is the output phase at that channel, and  $d$  is the relevant distance. Note that the sign is opposite from [22] because we use the  $\exp(+i\omega t)$  convention. In our case, we consider the lateral force between the resonator and the waveguide, hence  $d$  is the shortest separation between the resonator and the input waveguide, with  $F > 0$  being a repulsive force. In our case, there are two exit channels: the output port of the waveguide, and the loss; therefore, Eq. (3) becomes

$$F = -\frac{P_{out}}{\omega} \frac{\partial}{\partial d} \phi_{out} - \frac{P_{loss}}{\omega} \frac{\partial}{\partial d} \phi_{loss}. \quad (4)$$

Using Eqs. (1) and (2) and defining the transmission  $T = |t|^2$ , we can write

$$P_{out} = P_{in} T \quad (5)$$

$$\phi_{out} = \arg(t) \quad (6)$$

$$P_{loss} = P_{in}(1 - T) \quad (7)$$

$$\phi_{loss} = \arg(\eta) \quad (8)$$

where on the last equation, we assume the loss has the same phase as the resonator field. By evaluating Eq. (4), we obtain

$$F = -\frac{2P_{in}}{\omega} \left( \frac{\gamma_{om}\Delta}{\Delta^2 + (\gamma_0 + \gamma_e)^2} \right) - \frac{2P_{in}}{\omega} \left( \frac{g_{om}\gamma_e}{\Delta^2 + (\gamma_0 + \gamma_e)^2} \right) \quad (9)$$

where

$$g_{om} = \frac{\partial}{\partial d} \omega_0 \quad (10)$$

$$\gamma_{om} = \frac{\partial}{\partial d} \gamma_e. \quad (11)$$

The results here are the same as [13] but the derivation here is different. In both our derivation and the one in [13], the force occurs from the energy consideration, so this result is correct for general resonator-waveguide systems. Eq. (9) is related to how the electromagnetic energy inside the resonator changes as the waveguide-resonator distance varies: the first term of Eq. (9) corresponds to the change of the number of photons in the resonator, as it involves  $\gamma_{om}$  which is the derivative of the coupling rate with respect to  $d$ , while the second term of Eq. (9) corresponds to the change of the frequency or energy of each photon, as it involves  $g_{om}$  which is the derivative of the photon frequency with respect to  $d$  [13].

At a given frequency  $\omega$ , a stable equilibrium in the lateral direction occurs if there exists a resonator-waveguide separation  $d_0$  such that 1) the lateral force is zero at  $d_0$ , 2) the force is attractive for  $d > d_0$ , and 3) the force is repulsive for  $d < d_0$ . Therefore, to study the possibility for a stable optical equilibrium, we need to study how the sign of the force changes in  $d$  at a fixed frequency  $\omega$ . We will show analytically that in fact, at a fixed  $\omega$ , the force cannot change the sign as  $d$  varies. As a result, neither a stable nor unstable equilibrium point can be obtained from a single resonance.

To understand how the force changes with  $d$ , we need to know how  $\gamma_e$  and  $\omega_0$  explicitly vary with  $d$ . Because the resonator and the waveguide couple evanescently, we expect  $\gamma_e$  and  $\omega_0$  to vary with  $d$  as follows:

$$\gamma_e = \Gamma \exp(-\kappa d) \quad (12)$$

$$\omega_0 = \omega_\infty + \Omega \exp(-\kappa d) \quad (13)$$

where  $\kappa$  is the decaying constant.  $\Gamma$  is a positive constant.  $\omega_\infty$  is the resonance frequency in the absence of the waveguide.  $\Omega$  is a constant that can be positive, zero, or negative, depending on the resonance's type, mode, or polarization. Eqs. (12) and (13) will be verified numerically in the next section.

From Eqs. (12) and (13), we get

$$\gamma_{om} = -\kappa \Gamma \exp(-\kappa d) = -\kappa \gamma_e \quad (14)$$

$$g_{om} = -\kappa \Omega \exp(-\kappa d). \quad (15)$$

We see that  $\gamma_{om} < 0$ , hence the first term of Eq. (9), which is antisymmetric with respect to the resonant frequency, shows an attractive force on the lower-frequency side and a repulsive force on the higher-frequency side. However,  $g_{om}$  can be either positive or negative, so the second term of Eq. (9), which is symmetric around the resonant frequency, is repulsive if  $g_{om} < 0$  and attractive if  $g_{om} > 0$ . As a result, the total force has a lineshape that is asymmetric, with the dominant sign of force depending on the sign on  $g_{om}$ . This is illustrated in Fig. 2 where we assume an over-coupling regime ( $\gamma_e \gg \gamma_0$ ) to achieve a large resonance contribution to the optical force [10–13]. Note that the force peaks at neither  $\omega_0$  nor  $\omega_\infty$ .

At each waveguide-resonator separation  $d$ , we now solve for the frequency  $\omega_z$  where the force vanishes. Using Eqs. (9) and (12)-(15), and after a few lines of algebra, we obtain a remarkable result:

$$\omega_z = \omega_\infty. \quad (16)$$

In another word, independent of the waveguide-resonator separation, the force always vanishes at the frequency  $\omega_\infty$ , which is the resonance frequency of the resonator in the absence of the waveguide. Moreover, since  $\omega_z$  is independent of  $d$ , at each frequency, the force never changes sign as a function of  $d$ . Therefore, one cannot achieve an optical equilibrium in this system. Also, while the results here are derived for a travelling-wave single mode resonator, we note that the form of the force spectrum, i.e., Eq. (9), and the dependency of various resonance parameters on  $d$ , i.e., Eqs. (12)-(13), apply to a single-mode standing-wave resonator as well.

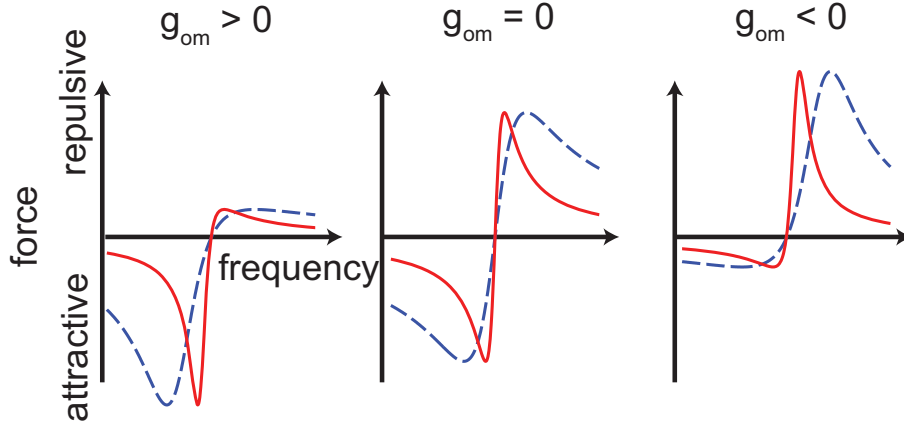


Fig. 2. The force lineshapes for three regimes of  $g_{om}$ . The dashed lines are at a smaller waveguide-resonator distance  $d$  than the solid lines. Notice that the force vanishes at the same frequency for different  $d$ .

Therefore, the main conclusion here, that one cannot achieve an optical equilibrium in the waveguide-resonator lateral force using a single-mode resonator, should hold in general.

Note that in this derivation, our result in Eqs. (9), (10), (11) is general for the waveguide-resonator force in any direction. For most of the paper, we specialize to the lateral force in Eqs. (12) and (13) where we specify the dependence of  $\gamma_e$  and  $\omega_0$  on the separation  $d$ . This consideration of the lateral force is usually sufficient for on-chip systems because the systems are usually restricted to move only in the lateral direction, while an out-of-plane motion (in the  $z$ -direction) and a longitudinal motion (in the  $x$ -direction) are negligible or impossible [7–9, 12]. Therefore, the lateral force in the  $y$ -direction is the main focus of our paper. However, using the same formalism we can also provide a study of an optical equilibrium in the  $z$ -direction. For this purpose, one can rewrite Eqs. (12) and (13) as

$$\gamma_e = \Gamma \exp(-\kappa \sqrt{d_f^2 + z^2}) \quad (17)$$

$$\omega_0 = \omega_\infty + \Omega \exp(-\kappa \sqrt{d_f^2 + z^2}) \quad (18)$$

where  $z$  is the out-of-plane relative position between the waveguide and the resonator, and  $d_f$  is the lateral waveguide-resonator separation at  $z = 0$ .  $\gamma_{om}$  and  $g_{om}$  are then the  $z$ -derivative of  $\gamma_e$  and  $\omega_0$  respectively. Combining these results with Eq. (9) gives the force in the  $z$ -direction ( $F_z$ ) of

$$F_z = -\frac{2P_{in}}{\omega} \frac{\gamma_e}{\Delta^2 + (\gamma_0 + \gamma_e)^2} \frac{(\omega - \omega_\infty)\kappa z}{\sqrt{d_f^2 + z^2}}. \quad (19)$$

This shows that  $z = 0$  is always an equilibrium position. And the  $z = 0$  position is stable if  $\omega > \omega_\infty$ , and unstable if  $\omega < \omega_\infty$ . For the longitudinal force in the  $x$ -direction, the momentum of the incident photons is transferred to the resonator, so the force on the resonator is in the  $+x$ -direction due to the optical scattering force.

## 2.2. Numerical example

As a concrete example to support the theory of a lateral force in the previous section, we consider a system comprising a racetrack-shaped ring resonator side-coupled to a waveguide as

shown in Fig. 1(a). We consider a two-dimensional example for simplicity; however, the result should apply to three-dimensional cases as well because our theory in the previous section applies to general waveguide-resonator systems. The waveguide and the resonator are made of silicon with the permittivity  $\epsilon_{Si} = 12.1$  and are surrounded by air with  $\epsilon_{air} = 1$ . Both the waveguide and the ring has a width of  $0.2 \mu\text{m}$ , which makes the waveguide single-mode. The radius of the semi-circular part of the resonator is  $1.5 \mu\text{m}$  and the straight section is  $1.1 \mu\text{m}$  long. The separation  $d$  between the resonator and the waveguide will be varied in the range of  $0.1 \mu\text{m} - 0.5 \mu\text{m}$ . The operating optical frequency corresponds to a free space wavelength near  $1.55 \mu\text{m}$ . We normalize the frequency to  $2\pi c/a$ , where  $c$  is the light speed in vacuum, and  $a = 1 \mu\text{m}$ . Hence a free space wavelength of  $1.55 \mu\text{m}$  corresponds to an angular frequency of  $0.65 \times 2\pi c/a$ . For simplicity, we consider a 2D system in TM mode (out-of-plane electric field and in-plane magnetic field). The simulation of this system is done using a finite-element frequency-domain method with a commercial software Comsol [23], and the optical force is calculated by integrating Maxwell's stress tensor.

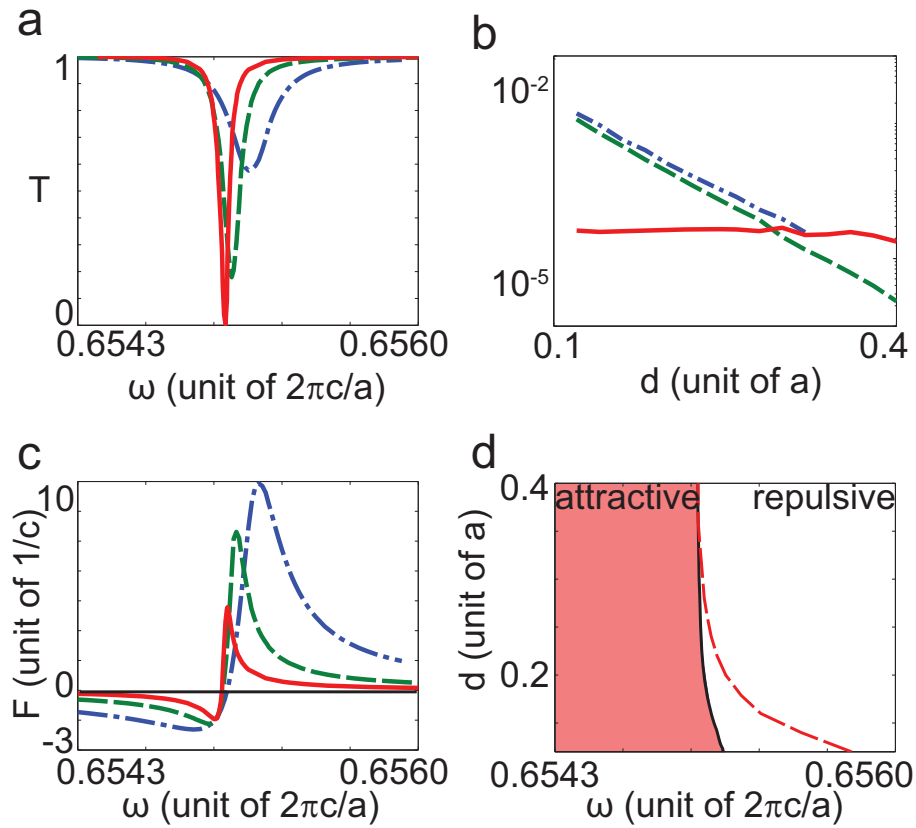


Fig. 3. Simulation result for the system in Fig. 1(a). (The length unit  $a = 1 \mu\text{m}$ .) (a)  $T$  as a function of  $\omega$  for  $d = 0.2 \mu\text{m}$  (dash-dotted line),  $d = 0.25 \mu\text{m}$  (dashed), and  $d = 0.3 \mu\text{m}$  (solid). (b) Fitted values of  $\gamma_0$  (solid),  $\gamma_e$  (dashed) and  $|\omega_0 - \omega_\infty|$  (dash-dotted) as a function of  $d$ . (c)  $F$  as a function of  $\omega$  for the same  $d$  as (a). (d) The sign of  $F$  as a function of  $\omega$  and  $d$  (shaded means attractive, white means repulsive). The dashed line is  $\omega_0$  as a function of  $d$ .

First, we verify that the coupled mode theory indeed applies by plotting the transmission

$T = |t|^2$  as a function of frequency  $\omega$  for several  $d$  in Fig. 3(a). We can see that the transmission spectrum has a symmetric dip as expected. We can also deduce that  $g_{om}$  is negative for this system because the resonance frequency decreases as  $d$  increases.

We then fit our parameters  $\gamma_e$ ,  $\gamma_0$  and  $\omega_0$  from the transmission spectrum using Eq. (2) for each value of  $d$ . We plot these parameters with respect to  $d$  in Fig. 3(b). We see that  $\gamma_0$  is constant in  $d$ , and  $\gamma_e$  and  $|\omega_0 - \omega_\infty|$  decay exponentially with approximately the same decay constant ( $21.8/a$  and  $21.3/a$  respectively), which verify the assumption of an evanescent coupling in Eqs. (12) and (13). We also found  $\omega_\infty = 0.655 \times 2\pi c/a$ .

Next, we verify the theoretical formula for the force spectrum (Eq. (9)) by examining the numerically computed force spectra as shown in Fig. 3(c). In this plot, the force per unit input power  $F$  is normalized to the unit of  $1/c$ . We can see that the force spectra are indeed asymmetric, with a small attractive force on the lower-frequency side and a large repulsive force on the higher-frequency side, as expected from Eq. (9) and the sign of  $g_{om}$ . Also, while the frequency where the maximum force occurs shifts significantly as  $d$  varies, we see that the force zero  $\omega_z$  does not change as  $d$  changes, as expected from our theory. Note that the numerical values of the force should remain approximately the same if we consider instead the three-dimensional case where both the waveguide and the resonator have an equal finite thickness in the  $z$ -direction. This is because the  $z$ -dependence of the local force and the local power density should be the same, so this  $z$ -dependence cancels out in the calculation of the force per input power.

To further emphasize that an optical equilibrium cannot be achieved with a single resonance, we plot the sign of  $F$  as a function of  $\omega$  and  $d$  in Fig. 3(d). We can see that in the regime where the resonance lineshape is nearly perfect Lorentzian, and hence the coupled mode theory for a single resonance is valid, we indeed observe near independence of the zero-force frequency as a function of  $d$ , in spite of the significant variation of the resonant frequency as a function of  $d$ . As a result, no equilibrium exists. At a smaller  $d$ , however,  $\omega_z$  changes slightly as  $d$  changes. This occurs because at a small  $d$ , the linewidth of the resonance is sufficiently large such that there is an additional contribution from the adjacent resonances, and as a result our assumption of having a single resonance no longer applies. Even in these cases where  $\omega_z$  does vary as a function of  $d$ , this deviation in  $\omega_z$  is much smaller than the linewidth at those  $d$ , and also smaller than the change in  $\omega_0$  as  $d$  changes, because the adjacent resonances are far away in frequencies. The analysis here therefore indicates that in order to achieve optical equilibrium in the waveguide-resonator system, one needs the resonator to support at least two resonances that are in a close proximity to each other in frequency.

### 3. Creating an optical equilibrium using two resonances

Building upon the understanding of the force behavior of a single resonance, in this section we will present an intuitive understanding of how an optical equilibrium can be created in a two-resonance system. In principle, one can express the force in a two-resonance system based on Eq. (9) approximately as

$$F = \sum_{i=1}^2 -\frac{2P_i}{\omega} \left( \frac{\gamma_{om,i}\Delta_i + g_{om,i}\gamma_{e,i}}{\Delta_i^2 + (\gamma_{0,i} + \gamma_{e,i})^2} \right) \quad (20)$$

where the parameters with subscript  $i$  are the parameters for each resonance. This expression assumes that the coherent interaction between the two resonances are weak such that we can neglect the cross-term when the power is calculated, which is an approximation. Nevertheless, as we will see in the numerical simulation, this expression does provide a reasonable explanation of the two-resonance case that we consider here. As a result, the exact formula of the force in a two-resonance case is very complicated and difficult to understand intuitively. Therefore, the goal of this section is to give an intuitive understanding of the lineshape of the force spectrum



for each resonance. Guided by this intuition, we then design structures that can achieve optical equilibrium in waveguide-resonator systems.

### 3.1. Theory

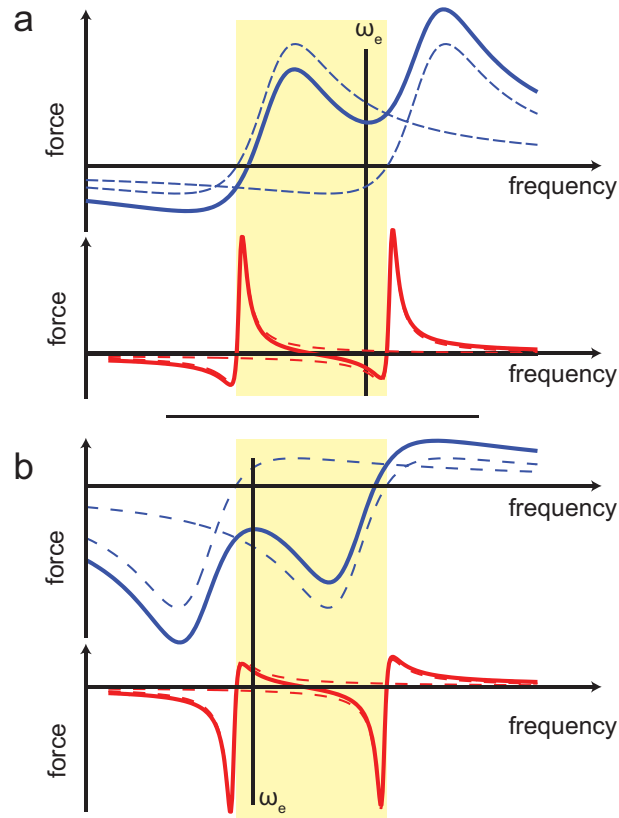


Fig. 4. (a) Force lineshape for a system with two  $g_{om} < 0$  resonances. The top plot is at smaller  $d$  than the bottom plot. The dashed lines are the contributions from each resonance. The solid lines are the total force. The frequency range between the zeros of force is shaded. (b) Same as (a) but with two  $g_{om} > 0$  resonances.

To construct a stable optical equilibrium, in Fig. 4(a), we consider a resonator system supporting two resonances, both with  $g_{om} < 0$ . We assume that the two resonances are close to each other in frequency. For each resonance, the frequency  $\omega_z$  where the force vanishes for each resonance does not vary as  $d$  changes, and the force is attractive for  $\omega < \omega_z$  and repulsive for  $\omega > \omega_z$ . Therefore, by assuming that the total force is the sum of the contributions from the two resonances, we see that the optical equilibrium can only occur at the frequencies between  $\omega_z$ 's of the two resonances (shaded region in Fig. 4), where the contributions from the two resonances are in opposite directions. Next, as shown in Fig. 2, a  $g_{om} < 0$  resonance, which has an asymmetric lineshape in its force spectrum, has a repulsive side with a larger peak amplitude, and an attractive side with a smaller peak amplitude. Also, as  $d$  increases, this repulsive peak narrows significantly, while the attractive peak changes less significantly in its width. With the arrangement in Fig. 4(a), the force between the two  $\omega_z$ 's is a sum of the contributions of the repulsive side of the lower frequency resonance, and the attractive side of the higher frequency

resonance. Therefore, the way each resonance varies with  $d$  as described above can lead to a change in the sign of force. The total force should change from repulsive to attractive as  $d$  increases, creating a stable optical equilibrium. With a similar argument, we can see that a system with two  $g_{om} > 0$  resonances, as shown in Fig. 4(b), results in an unstable optical equilibrium.

Guided by the intuition above, in the remaining parts of this section, we provide two concrete examples that exhibit a stable optical equilibrium.

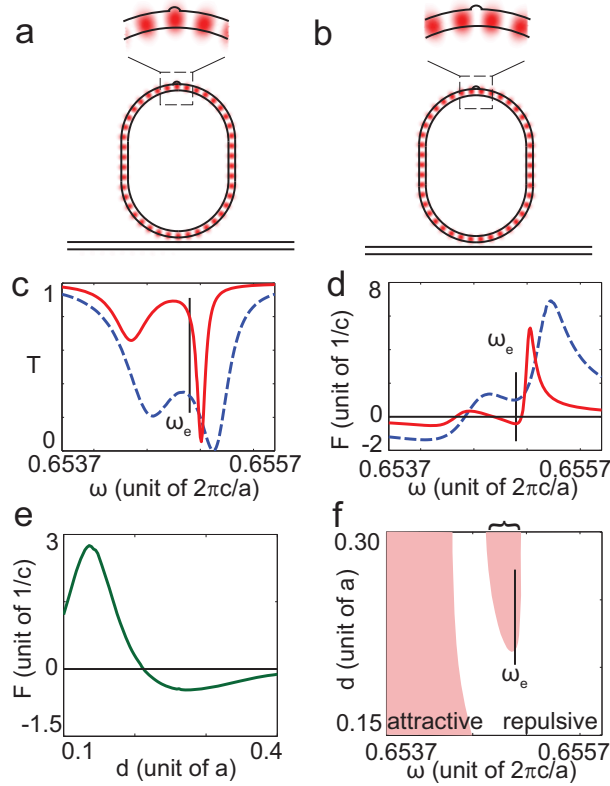


Fig. 5. (a) and (b) the schematic of the ring resonator in Fig. 1(b) with a small circular bump (radius of  $0.06\mu\text{m}$ ). The red color shows the light intensity of the two modes. (c)  $T$  and (d)  $F$  as a function of  $\omega$  for  $d = 0.20\mu\text{m}$  (dashed line), and  $d = 0.32\mu\text{m}$  (solid). (e)  $F$  as a function of  $d$  at  $\omega = \omega_e \equiv 0.655 \times 2\pi c/a$ . (f) The sign of  $F$  as a function of  $\omega$  and  $d$  (shaded means attractive, white means repulsive). The bracket denotes the frequency range where an optical equilibrium occurs.

### 3.2. First example: a bumped ring resonator

In the first example, we modify the ring resonator in Sec. 2 by adding a small circular bump, with a radius of  $0.06\mu\text{m}$ , at the top of the resonator as shown in Figs. 5(a)-(b). The ring resonator in Sec. 2 supports a pair of degenerate travelling-wave resonances. An incident wave in the waveguide from one side couples only to one of these two travelling wave resonances, and as a result the system can be described as a single-mode resonator. In the presence of the bump, the two travelling wave resonances in the ring couple to each other to form two standing wave resonances, with intensity patterns shown in Fig. 5(a) and Fig. 5(b). We see that one of the standing wave resonances have an intensity node, while the other has an intensity anti-node,

at the position of the bump. Both resonances now couple to the waveguide, as can be seen in the transmission spectra for a range of the waveguide-resonator separation  $d$  at Fig. 5(c). All these spectra exhibit two resonance dips. Since both resonances shift to smaller frequencies as  $d$  increases, we deduce that  $g_{om} < 0$  for both resonances. Therefore, the resonances in this system have the characteristics of what is required in Fig. 4(a).

The force spectra for this system, for  $d = 0.18 \mu\text{m}$ , and  $d = 0.25 \mu\text{m}$ , were shown in Fig. 5(d). We see that around the frequency  $\omega_e = 0.6549 \times 2\pi c/a$  (marked with the vertical line), the system indeed exhibit a stable optical equilibrium, with the force changes from repulsive to attractive, at a fixed frequency, as  $d$  increases. To emphasize this fact, we plot the force as a function of  $d$  at the frequency  $\omega_e$  in Fig. 5(e). This clearly shows a stable optical equilibrium at  $d_0 = 0.21 \mu\text{m}$ ; at this frequency, as  $d$  moves away from  $d_0$ , the optical force always points towards  $d = d_0$ . We also plot the sign of  $F$  as a function of  $\omega$  and  $d$  in Fig. 5(f), which shows that there exists a stable optical equilibrium over the frequency range of  $0.6546 \times 2\pi c/a$  to  $0.6550 \times 2\pi c/a$  (shown as the bracket in the figure).

In comparing Figs. 5(c) and 5(d), we see that in this system, at  $\omega_e$ , at smaller  $d$ , the repulsive force contribution from the lower-frequency resonance dominates over the attractive force contribution of the higher-frequency resonance. On the other hand, as  $d$  increases, the contribution from the lower-frequency resonance decays faster than the higher-frequency resonance. As a result, the force changes from repulsive to attractive as  $d$  increases, creating a stable optical equilibrium. In this case, the fast decay of the contribution of the lower-frequency resonance comes not only from the fact that it has  $g_{om} < 0$  and therefore has a fast-narrowing repulsive peak as indicated in Fig. 4(a), but also that in this case, the lower-frequency resonance enters the under-coupling regime (where the force is small [10–13]) at a smaller  $d$  than the higher-frequency resonance. This fact can be deduced from the plot of  $T$  in Fig. 5(c) because in an under-coupling regime, the dip in  $T$  spectrum becomes shallower as  $d$  increases.

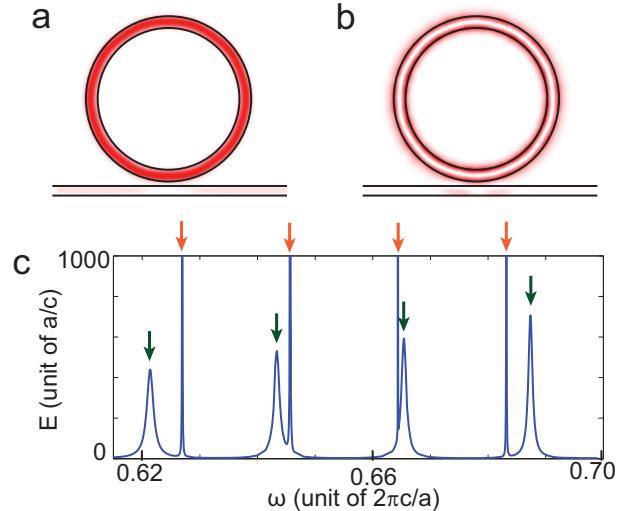


Fig. 6. The schematic of the two-mode ring resonator with an inner radius of  $1.80 \mu\text{m}$  and an outer radius of  $2.15 \mu\text{m}$ . The red color shows the light intensity. (a) the first-order mode. (b) the second-order mode. (c) The ratio of the energy inside the resonator to the input power ( $E$ ) as a function of  $\omega$  at  $d = 0.18 \mu\text{m}$ . Dark green arrows denote the first-order modes. Light orange arrows denote the second-order modes.

### 3.3. Second example: using two families of traveling-wave modes in a single ring resonator

In this example, we use a thick ring resonator (an inner radius of  $1.80 \mu\text{m}$  and an outer radius of  $2.15 \mu\text{m}$ ). This resonator can support two families of travelling-wave modes, with the intensity patterns shown in Fig. 6(a)-(b). The first-order modes (Fig. 6(a)) have no intensity node inside the ring. The second-order modes (Fig. 6(b)) have an intensity node inside the ring. By studying the force lineshape of each mode (not plotted), we found that the first-order modes have  $g_{om} \approx 0$  while the second-order modes have  $g_{om} < 0$ . The positions of these two families of modes in frequency are shown in Fig. 6(c), where the ratio of the energy inside the ring to input power ( $E$ ), in the unit of  $a/c$ , is plotted as a function of frequency at  $d = 0.18 \mu\text{m}$ . We can see that in the two frequency ranges of  $0.642 \times 2\pi c/a$  to  $0.648 \times 2\pi c/a$  and  $0.663 \times 2\pi c/a$  to  $0.668 \times 2\pi c/a$ , there are two modes, one from each of the two families, that overlap in frequency. Based on the arguments above we will therefore seek to find an optical equilibrium in these ranges. Moreover, the relative positions in the frequency of the two modes are different in each range; in the first range, the second-order mode is at a higher frequency, but in the second range, the first-order mode is at a higher frequency. Therefore, these two ranges of frequency provide an interesting contrast of how different resonances affect the creation of an optical equilibrium.

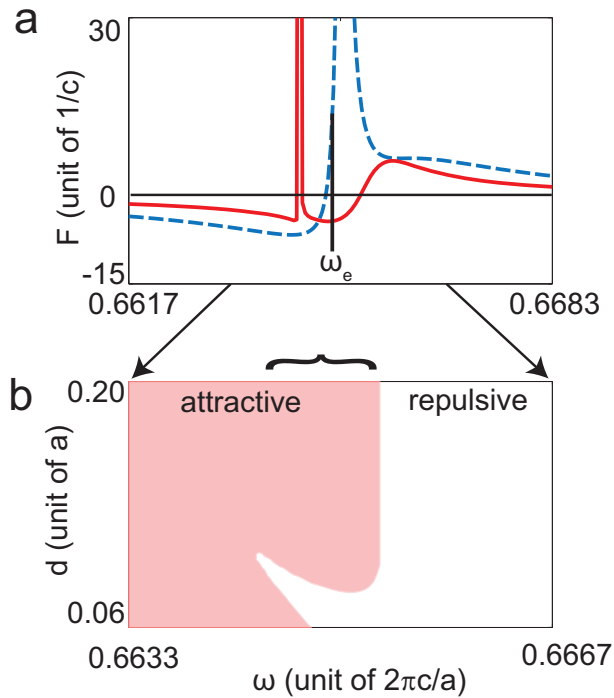


Fig. 7.  $F$  for a system in Fig. 6 near the frequency of  $0.665c/a$ . (a)  $F$  as a function of  $\omega$  for  $d = 0.06 \mu\text{m}$  (dashed line), and  $d = 0.1 \mu\text{m}$  (solid). (b) The sign of  $F$  as a function of  $\omega$  and  $d$  (shaded means attractive, white means repulsive).  $\omega_e = 0.655 \times 2\pi c/a$ . The bracket denotes the frequency range where an optical equilibrium occurs.

First, we consider the frequency range of  $0.663 \times 2\pi c/a$  to  $0.668 \times 2\pi c/a$ , where the second-order mode is at a lower frequency than the first-order mode as shown in Fig. 7(a). In this system, the  $g_{om} < 0$  resonance has the lineshape that is very asymmetric with a very high repulsive peak; therefore, the contribution from this repulsive peak near  $\omega_e = 0.665 \times 2\pi c/a$

decreases significantly as  $d$  increases. This drop in the repulsive force, combining with the contribution from the attractive side in the lineshape of the high-frequency first-order mode, creates a stable optical equilibrium. This is shown in Fig. 7(a) where, near  $\omega_e$ , the force changes from repulsive to attractive as  $d$  increases. The plot of  $F$  as a function of  $\omega$  and  $d$  in Fig. 7(b) also shows a stable optical equilibrium occurring in the frequency range shown by the bracket.

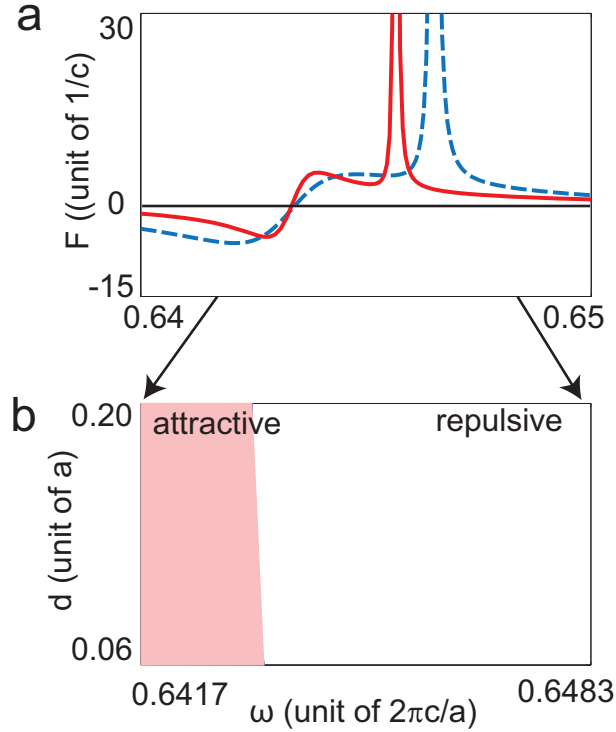


Fig. 8.  $F$  for a system in Fig. 6 near the frequency of  $0.645c/a$ . (a)  $F$  as a function of  $\omega$  for  $d = 0.06 \mu\text{m}$  (dashed line), and  $d = 0.1 \mu\text{m}$  (solid). (b) The sign of  $F$  as a function of  $\omega$  and  $d$  (shaded means attractive, white means repulsive).

Next, we consider the frequency range of  $0.642 \times 2\pi c/a$  to  $0.648 \times 2\pi c/a$ , where the second-order mode is at a higher frequency than the first-order mode (Fig. 8). In this case, the  $g_{om} < 0$  resonance (second-order mode) is at a higher frequency. Because the strong repulsive contribution of this resonance does not lie between the two resonances, this system lacks the large swing in the force that is required for the change in the sign of the force. As a result, an optical equilibrium does not occur in this system. This is shown in Fig. 8(a) and 8(b), where no change in the sign of the force is observed.

Finally, we point out that, even though the existence of an optical equilibrium depends mainly on  $g_{om}$ , which is the derivative of the coupling  $\gamma_e$  with respect to  $d$ , the resonator with low intrinsic loss  $\gamma_0$  is still desired even though  $\gamma_0$  does not directly affect the existence of an optical equilibrium. This is because the magnitude of the optical force decays quickly in  $d$  if  $d$  is large enough that  $\gamma_0 > \gamma_e$  (under-coupling regime) [11]. Therefore, for the optical equilibrium to have a significant restoring optical force,  $\gamma_0$  should be low enough that the system is still in the over-coupling regime at the equilibrium distance.

#### **4. Summary and conclusions**

In summary, we studied the optical equilibrium in the lateral optical force in resonator-waveguide system. We proved analytically and numerically that an optical equilibrium cannot occur in a single-resonance system. We also provide an intuitive picture, supported by numerical simulations, on the conditions for creating optical equilibrium in two-resonance systems. We believe our work will be useful in the development of self-tuned and robust optical circuits based on optomechanics.

#### **Acknowledgments**

This work is supported by an AFOSR-MURI program on Integrated Hybrid Nanophotonic Circuits (Grant No. FA9550-12-1-0024).